Fluorescence Detection of Single-Nucleotide Polymorphisms with a Single, Self-Complementary, Triple-Stem DNA Probe

ARTICLE *in* ANGEWANDTE CHEMIE INTERNATIONAL EDITION · JUNE 2009

Impact Factor: 11.26 · DOI: 10.1002/anie.200900369 · Source: PubMed

7 AUTHORS, INCLUDING:

Yi Xiao
Florida International University
67 PUBLICATIONS **6,844** CITATIONS
SEE PROFILE

Xinhui Lou
Capital Normal University
35 PUBLICATIONS **1,124** CITATIONS
SEE PROFILE

Ryan J White
University of Maryland, Baltimore County
44 PUBLICATIONS **1,482** CITATIONS
SEE PROFILE

Published in final edited form as:
Angew Chem Int Ed Engl. 2009 June 2; 48(24): 4354–4358. doi:10.1002/anie.200900369.

Fluorescence Detection of Single Nucleotide Polymorphisms via a Single, Self-Complementary, Triple-stem DNA Probe**

Dr. Yi Xiao,
Materials Department, Department of Mechanical Engineering, University of California, Santa Barbara, Santa Barbara, CA 93106 (USA), Fax: (+1) 805-893-8651

Kory J.I. Plakos,
Materials Department, Department of Mechanical Engineering, University of California, Santa Barbara, Santa Barbara, CA 93106 (USA), Fax: (+1) 805-893-8651

Dr. Xinhui Lou,
Materials Department, Department of Mechanical Engineering, University of California, Santa Barbara, Santa Barbara, CA 93106 (USA), Fax: (+1) 805-893-8651

Dr. Ryan J. White,
Department of Chemistry, University of California, Santa Barbara, Santa Barbara, CA, 93106 (USA)

Dr. Jiangrong Qian,
Materials Department, Department of Mechanical Engineering, University of California, Santa Barbara, Santa Barbara, CA 93106 (USA), Fax: (+1) 805-893-8651

Prof. Kevin W. Plaxco, and
Department of Chemistry, University of California, Santa Barbara, Santa Barbara, CA, 93106 (USA)

Prof. H. Tom Soh
Materials Department, Department of Mechanical Engineering, University of California, Santa Barbara, Santa Barbara, CA 93106 (USA), Fax: (+1) 805-893-8651, tsoh@engr.ucsb.edu

Abstract

We describe a single-step, single-component, fluorescence-based method of detecting single nucleotide polymorphisms at room temperature without exogenous reagents. The sensor is comprised of a single, self-complementary DNA strand forming a triple-stem structure, which undergoes a large conformational change only upon binding to perfectly-matched targets, resulting in a significant increase in fluorescence.

Keywords

DNA; Single nucleotide polymorphisms; Fluorescence; Triple-stem; Self-complementary

Single nucleotide polymorphisms (SNPs) can serve as an important indicator of genetic predisposition towards disease states or drug responses,[1,2a] and detection of rare base

**This work was supported by the Office of Naval Research (N00014-08-1-0469), the National Institutes of Health (R21 EB008215) and by the Institute for Collaborative Biotechnologies through grant DAAD19-03-D-0004 from the U.S. Army Research Office.

Correspondence to: H. Tom Soh.

Supporting information for this article is available on the WWW under http://www.angewandte.org or from the author.

substitutions within populations of DNA molecules is essential for studying effects of DNA damage and for pool screening for SNPs.[2b] There is thus an urgent need for technologies suitable for sensitive, high-throughput SNP detection.[3] Ideally, these would be single-step, reagentless, room temperature assays, suitable for clinical and research use and compatible with microarray technologies for massively analysis.[4]

Unfortunately, current technologies satisfy only some of these requirements. For example, enzymatic SNP detection methods, such as endonuclease digestion,[5,6] primer extension[7] and ligation assays,[8] are very sensitive and specific even at room temperature, but are complex, multi-step techniques that often require separation of the resultant products in order to determine the presence of the target sequence. These limitations have motivated the development of simpler fluorescence-based assays utilizing molecular beacons,[9-11] binary probes,[12,13] forced intercalation of thiazole orange (FIT) probes[14] and base-discriminating fluorescent (BDF) probes. [15]

Molecular beacons (MBs) are stem-loop oligonucleotides with self-complementary 5’ and 3’ ends that bring a fluorophore-quencher pair into close proximity in the absence of target. Hybridization to a complementary target disrupts the stem-loop, segregating the pair and thereby inducing a large increase in fluorescence.[16] MBs are well-suited for rapid SNP detection, as they allow reagentless and quantitative analysis without the need for separation steps.[9-10,16-19] However, their reliance on melting temperature of probe-target duplexes as the basis for mismatch discrimination limits potential targets to those whose melting temperatures can be distinguished via precise temperature control. With a few exceptions,[20,21] MBs typically do not perform well at room temperature without significant, empirical optimization of their thermodynamics.[22]

Binary probe assays avoid these limitations and enable SNP analysis at room temperature.[8,12-13,23-25] These utilize a pair of non-identical DNA probes that form relatively short (7- to 10-nucleotide) duplexes at sites adjacent to a target sequence. Signal detection is achieved via ligation reaction,[8] fluorescence[23] or colorimetric[24] readouts, or by resonance energy transfer.[25] These short hybrids are very sensitive to mismatches, and can readily distinguish single nucleotide substitutions, rendering the approach specific, sensitive and reliable. However, the approach requires the addition of multiple exogenous reagents. Other alternatives include thiazole orange-modified FIT probes[14] or BDF probes[15] which are modified single-stranded DNAs that produce only weak fluorescence in the absence of target, but emit strong fluorescence upon target recognition. However, their specificity for SNP detection is highly dependent on linker length, conjugation site and the sequence of the mismatched base-pairs. Thus, there remains a need for simple and efficient room temperature SNP assays without significant probe optimization.

Towards this end, we present here a strategy that combines advantages of MBs and binary probes in a single triple-stem DNA structure to achieve robust single-step SNP detection in a homogeneous, room temperature system without exogenous reagents. This probe produces negligible signal in the presence of single-base mismatched targets, but hybridization to a perfectly-matched target induces a significant conformational change that results in a large increase in fluorescence signal (Figure 1). Importantly, the triple-stem probe architecture allows tuning of its sensitivity and selectivity towards specific target sequences over a wide temperature range.

The triple-stem DNA based SNP sensor consists of a single 68-base DNA strand (**1**) that has been modified with a CAL Fluor Red 610 (FR610) fluorophore at the 3’ terminus and a Black Hole Quencher (BHQ) at an internal position. At room temperature, the probe self-hybridizes into three separate, seven base-pair (bp) Watson-Crick stems that form a

discontinuous, 21-base double helix[26] (Figure 1A, left). In the absence of target, this relatively rigid triple-stem structure holds the fluorophore in close proximity to the quencher, resulting in very limited fluorescence (Figure 1B). Upon hybridizing to a perfectly-matched 17-nucleotide target (PM; **2**) the triple-stem structure is disrupted, separating the fluorophore-quencher pair (Figure 1A) and inducing a 29-fold increase in emission intensity (Figure 1B). In contrast, when the probe is challenged with target containing a single-base mismatch in the middle of the sequence (1MM; **3**), we observe only a 1.3-fold increase in emission intensity, even at a four-fold higher concentration (Figure 1B); a two-base mismatched target (2MM; **4**) does not produce any detectable increase in fluorescence (Figure 1B). An important feature of our probe structure is that its design requires minimal optimization. As an example, we synthesized a second triple-stem probe (**5**) with an A-to-G substitution at position 39 (from 5' end). The sequence of this probe now perfectly matches the 1MM target (**3**) and thus is mismatched with the PM target (**2**). As expected, we obtained a large increase (26-fold) in emission intensity upon addition of the 1MM target (**3**), and minimal signal gain was observed with the PM target (**2**) (see Figure S1 in Supporting Information).

The thermodynamic stability of both the probe itself and the probe-target duplexes enables remarkable specificity for SNPs over a wide temperature range up to 60 °C. The triple-stem probe is assumed to exist in three different phases in the presence of targets[27]: phase 1 as a target/probe duplex, phase 2 as a folded probe, and phase 3 as a random coil (Figure 2A). At low temperatures, the probe hybridizes with the PM target (phase 1), giving rise to significantly increased fluorescence (Figure 2B). As temperature increases, the duplex is destabilized and the released probe apparently re-folds into its native structure (phase 2), resulting in significantly diminished fluorescence. For the PM target, the transition from target-probe duplex to self-complementary triple-stem structure occurred at 65 °C. At temperatures above 82 °C, the folded probe melted into random coils (phase 3) in which quenching efficiency is reduced, leading to a small increase in fluorescence. In contrast, little fluorescence was observed for 1MM or 2MM targets at low temperatures (Figure 2B), and the signals in the presence of no target, PM and mismatched targets merged at higher temperatures.

In an effort to investigate the kinetic response of the triple-stem probe, we performed time-resolved measurements using 1 μM PM target or and 4 μM mismatched targets. We define the single-mismatch discrimination factor as the ratio of the net fluorescence intensity obtained with the PM target to that obtained with 1MM after subtraction of background fluorescence; thus, a larger discrimination factor is indicative of greater specificity. Upon addition of the PM target to a solution of native, quenched probe, we observed an exponential rise in fluorescence over time (see Figure S2 in Supporting Information). In contrast, almost no signal change was observed with mismatched targets (Figure S2). The equilibration time constant for the PM target is ~78 min, which is similar to that observed for binary probe methods[8,12] but slower than that of MBs.[9-10] This presumably reflects the stability of the triple-stem structure (T_m = 80.2 °C).[28-29] However, this method compares favorably with enzyme-mediated SNP detection methods[5-8]: a discrimination factor of 16 was obtained after 30 min, with signal saturation occurring at a discrimination factor of 28 after 3 hours (Figure S2). Moreover, we did not observe any signal difference between samples that had been equilibrated for three hours (Figure 2C, lanes 1-3) and samples that had been equilibrated for three days (Figure 2C, lanes 4-6), which strongly suggests we are operating in the equilibrium limit. Likewise, polyacrylamide gel electrophoresis indicates that equilibration is complete within 3 hours and that only perfectly-matched targets produce the 85-bp band corresponding to the probe-target duplex (Figure 2C, lanes 2 and 5). Under the conditions employed here, the calculated hybridization

efficiency of our system is ~45% (Figure 2C, lanes 1 and 2; lanes 4 and 5), which confirms that target concentration plays an important role in hybridization efficiency.

Titration experiments confirmed that the triple-stem probe displays remarkable specificity for perfectly-matched targets, with minimal response to even substantially higher concentrations of mismatched targets. The probe achieved a peak discrimination factor of 30 when titrated with the PM target (Figure. 2D, inset); in contrast, we observed only a 1.5-fold increase in fluorescence intensity in the presence of 4 μM 1MM target (see Figure S3 in supporting information). We observed a high degree of discrimination over a wide target concentration range up to 300 μM (data not shown); for example, we achieved a discrimination factor of 4 in a comparative analysis with 32 nM of each target, and a discrimination factor of 5 for 125 nM PM target versus 4 μM 1MM target (Figure 2D). The titration curve shows the nonlinear hyperbolic relationship between DNA hybridization efficiency and target concentration;[30-32] it is reminiscent of an active site titration wherein the PM target has high affinity and the 1MM target has low affinity.

To confirm the general applicability of the triple-stem probe, we tested its capacity to discriminate against mismatched bases at different positions within the PM target. We obtained discrimination factors ranging from 5.6 to 28.4 (Table 1); the highest level of discrimination occurred with duplexes containing a C/C mismatch, while the lowest was observed with an A/A mismatch. This is consistent with previous findings that the thermodynamics of mismatches depend on the identity of the mismatched base-pair as well as the identity of its near neighbors.[33,34] The triple-stem probe also displayed excellent discrimination for shorter (15-base) and longer (19-base) targets (see Table S1 in Supporting Information).

We believe that the exceptional specificity of the triple-stem probe originates from its thermodynamic stability; at room temperature, the 21-bp discontinuous duplex in the probe is less stable than the continuous 17-bp PM target-probe duplex. Therefore, the presence of the PM target efficiently disrupts the native probe structure, resulting in probe-target hybridization. In contrast, the native triple-stem structure is markedly more stable than duplexes containing a single mismatch, inhibiting 1MM target-probe hybridization.

To better understand the thermodynamic basis for this phenomenon, we used van't Hoff plots[35] to investigate the enthalpy and entropy changes describing the phase transition between phase 2 and 3 ($\Delta H_{2\rightarrow3}^0$ and $\Delta S_{2\rightarrow3}^0$), and found that the triple-stem probe undergoes large enthalpy and entropy changes ($\Delta H_{2\rightarrow3}^0 = 30 \pm 3$ kcal/mol; $\Delta S_{2\rightarrow3}^0 = 85 \pm 9$ cal/(mol·K)).

To construct the free energy diagram [27,35] for the three phases of our probe, we measured the enthalpy and entropy changes associated with the dissociation of duplexes with PM and 1MM targets. The plot displays the expected linear relationship between the inverse of melting temperature ($1/T_m$) and R $\ln(T_0 - 0.5P_0)$ (where R is the gas constant, T_o is the initial concentration of targets, and P_0 is the initial concentration of probe) (Figure 3A). The enthalpies and entropies of the transitions from phase 1 to 2 ($\Delta H_{1\rightarrow2}^0$ and $\Delta S_{1\rightarrow2}^0$) were determined from these linear relationships, and the T_m was determined using a series of solutions containing 50 nM of probe and various excess concentrations of 17-base targets. A three-fold difference in $\Delta H_{1\rightarrow2}^0$ and $\Delta S_{1\rightarrow2}^0$ was obtained between the PM target ($\Delta H_{1\rightarrow2}^0 = 90 \pm 3$ kcal/mol; $\Delta S_{1\rightarrow2}^0 = 240 \pm 17$ cal/(mol·K)) and 1MM target ($\Delta H_{1\rightarrow2}^0 = 32 \pm 2$ kcal/mol; $\Delta S_{1\rightarrow2}^0 = 76 \pm 9$ cal/(mol·K)), indicating that mismatched targets dissociate from the triple-stem probe more readily. Based on the measured enthalpy and entropy changes in the three phases, the thermodynamic stability associated with our triple-stem probe has the following hierarchy: PM target-probe hybrid $\gg$ 1MM target-probe hybrid $\approx$ probe self-

hybridization. The dissociation of the probe-target duplex results in an entropy gain when the duplex dissociates and an enthalpy loss when the secondary structures reform in the probe. Because the triple-stem probe undergoes significant self-reorganization upon dissociation (or formation) of probe-target duplexes, both the enthalpic and entropic contributions to the free energy of the probe-target dissociated state, especially in the presence of a mismatched base pairing, lead to significantly improved specificity.

To further elucidate the origins of probe specificity, we constructed free energy diagrams of the probe in equilibrium with its targets as a function of temperature ($\Delta G^0 = \Delta H^0 - T\Delta S^0$) (Figure 3B). Here, phase 3 was chosen as the reference state ($\Delta G_3^0 = 0$), because under these conditions the probe and targets form random coils. The ΔG^0 values for phase 2 and 3 are calculated according to the reported equations.[27] The predominant phase at each temperature is the phase with the lowest free energy. It is clear from the free energy diagram that the transition range over which the probe-PM duplex is stable and the probe-1MM duplex is unstable is significant (Φ = 43.6 °C). Our triple-stem probe is therefore capable of SNP discrimination over a wide temperature range.

We have reported here a reagentless, single-step, fluorescence-based method for rapid and accurate SNP detection, based on target binding-induced conformational change of a single, self-complementary DNA probe. Our probe can easily discriminate 62.5 nM perfectly-matched target against as much as 4 μM single-base mismatched target (a 64-fold excess) within 30 minutes at room temperature; in contrast, a comprehensive study revealed that conventional MBs typically achieve robust single mismatch discrimination at 60-70°C. [36,37] Our probe design shares similarity with tripartite molecular beacons,[38] and is elegantly simple—it is only a single, chemically-modified DNA strand. We note that the current detection limit of our method is ~10 nM (500 ng/μl), which preempts direct analysis of genomic DNA—the concentration of genomic DNA obtained in standard phenol:chloroform extractions is typically ~30 ng/μl.[39] Thus, similar to most MB approaches, PCR amplification is necessary prior to the detection.

Importantly, the design of the triple-stem probe is straightforward and requires negligible optimization to achieve the specific SNP detection reported here. This offers a advantage for multi-target, parallel analysis over conventional MBs, which require significant optimization for each target sequence. Taken with the observation that both DNA or RNA probes can form triple-stem structures,[26] and that our probe can be covalently surface-linked onto a solid-phase substrate, we believe the approach may provide a scalable strategy for high-throughput SNP discovery and analysis via microarray technologies.

Experimental Section

Materials

All chemicals were purchased from Sigma-Aldrich, Inc. (Saint Louis, MO, USA) and used without further purification. The fluorophore/quencher-labeled DNA oligonucleotides were synthesized by Biosearch Technologies, Inc. (Novato, CA, USA), purified by C18 HPLC, and confirmed by mass spectrometry (see Figure S4 and Figure S5 in supporting information). The sequences of these modified oligomers are: (**1**) 5'-AGGCTGGATTTTTTATTTACCTTTTTTTAGGTAAA-(BHQ)A-CG**A**CGGCCAGCCTTTTTTTTTTTTTCCGTCGT-T(Cal Fluor 610) -3'; (**5**) 5'-AGGCTGGATTTTTTATTTACCTTTTTTTAGGTAAA-(BHQ)A-CG**G**CGGCCAGCCTTTTTTTTTTTTTCCGTCGT-T(Cal Fluor 610) -3'

The perfectly-matched and mismatched DNA targets were purchased from Integrated DNA Technologies Inc. (Coralville, IA, USA), and were purified by HPLC. The sequences of

these DNA targets are: 15-base DNA targets: PM target: 5'-CTGGCCGTCGTTTTA-3'; 1MM target: 5'-CTGGCCGT**A**GTTTTA-3'; 17-base DNA targets: PM target: (**2**) 5'-GCTGGCCGTCGTTTTAC-3'; 1MM target: (**3**) 5'-GCTGGCC**C**TCGTTTTAC-3'; 2MM target: (**4**) 5'-GCTGGCC**CC**CGTTTTAC-3'; 19-base DNA targets: PM target: 5'-GGCTGGCCGTCGTTTTACC-3'; 1MM target: 5'-GGCTGGCC**C**TCGTTTTACC-3'.

Fluoresence experiments

Experimental details of fluorescence denaturation experiments, kinetic experiments, determination of melting temperatures (T_M) and measurement of discrimination factors are provided in supporting information.

Polyacrylamide gel electrophoresis

The samples including the triple-stem probe (0.5 μM) only, or hybridized with 1.0 μM 17-base PM target, or 4 μM 17-base 1MM targets (100 μl as a total reaction volume) that have been equilibrated for three hours and three days were analyzed on a 10% PAGE–TBE gel (Ready gel, Bio-Rad laboratories, CA, USA) at 120V for 60 minutes. The gel was stained for 20 minutes with Gel star nucleic acid stain (Lonza, Rockland, ME, USA) and imaged using with a KODAK Gel Logic EDAS 200 Digital Imaging System (NY, USA).

Supplementary Material

Refer to Web version on PubMed Central for supplementary material.

References

1. Suh Y, Vijg J. Mutat Res-Fundam Mol Mech Mutagen 2005;573:41–53.
2. (a) Schafer AJ, Hawkins JR. Nature Biotechnol 1998;16:33–39. [PubMed: 9447590] (b) Luo JD, Chan EC, Shih CL, Chen TL, Liang Y, Hwang TL, Chiou CC. Nucleic Acids Res 2006;34:e12. [PubMed: 16432256]
3. Fan JB, Chen XQ, Halushka MK, Berno A, Huang XH, Ryder T, Lipshutz RJ, Lockhart DJ, Chakravarti A. Genome Res 2000;10:853–860. [PubMed: 10854416]
4. Gunderson KL, Steemers FJ, Lee G, Mendoza LG, Chee MS. Nature Genet 2005;37:549–554. [PubMed: 15838508]
5. Youil R, Kemper BW, Cotton RGH. Proc Natl Acad Sci USA 1995;92:87–91. [PubMed: 7816853]
6. Livak KJ, Marmaro J, Todd JA. Nature Genet 1995;9:341–342. [PubMed: 7795635]
7. Nelson NC, Hammond PW, Matsuda E, Goud AA, Becker MM. Nucleic Acids Res 1996;24:4998–5003. [PubMed: 9016672]
8. (a) Landegren U, Kaiser R, Sanders J, Hood L. Science 1988;241:1077–1080. [PubMed: 3413476] (b) Ficht S, Mattes A, Seitz O. J Am Chem Soc 2004;126:9970–9981. [PubMed: 15303871] (c) Sando S, Kool ET. J Am Chem Soc 2002;124:9686–9687. [PubMed: 12175209]
9. Kostrikis LG, Tyagi S, Mhlanga MM, Ho DD, Kramer FR. Science 1998;279:1228–1229. [PubMed: 9508692]
10. Kostrikis LG, Shin S, Ho DD. Mol Med 1998;4:443–453. [PubMed: 9713823]
11. Grossmann TN, Roglin L, Seitz O. Angew Chem Int Ed 2007;46:5223–5225.
12. Xu YZ, Karalkar NB, Kool ET. Nature Biotechnol 2001;19:148–152. [PubMed: 11175729]
13. Kolpashchikov DM. J Am Chem Soc 2005;127:12442–12443. [PubMed: 16144363]
14. (a) Köhler O, Seitz O. Chem Commun 2003:2938–2939. (b) Köhler O, Venkatrao D, Jarikote DV, Seitz O. ChemBioChem 2005;6:69–77. [PubMed: 15584015] (c) Socher E, Jarikote DV, Knoll A, Röglin L, Burmeister J, Seitz O. Anal Biochem 2008;375:318–330. [PubMed: 18249184]
15. (a) Okamoto A, Kanatani K, Saito I. J Am Chem Soc 2004;126:4820–4827. [PubMed: 15080686] (b) Okamoto A, Tainaka K, Ochi Y, Kanatani K, Saito I. Mol Biosyst 2006;2:122–126. [PubMed: 16880929]

16. Dubertret B, Calame M, Libchaber AJ. Nature Biotechnol 2001;19:365–370. [PubMed: 11283596]
17. Tyagi S, Kramer FR. Nature Biotechnol 1996;14:303–308. [PubMed: 9630890]
18. Nutiu R, Li YF. Nucleic Acids Res 2002;30:e94. [PubMed: 12235396]
19. Hwang GT, Seo YJ, Kim BH. J Am Chem Soc 2004;126:6528–6529. [PubMed: 15161261]
20. Socher E, Bethge L, Knoll A, Jungnick N, Herrmann A, Seitz O. Angew Chem Int Ed 2008;47:9555–9559.
21. French DJ, Archard CL, Brown T, McDowell DG. Mol Cell Probes 2001;15:363–374. [PubMed: 11851380]
22. Kwok PY. Annu Rev Genomics Hum Genet 2001;2:235–258. [PubMed: 11701650]
23. Kolpashchikov DM. J Am Chem Soc 2006;128:10625–10628. [PubMed: 16895431]
24. Kolpashchikov DM. J Am Chem Soc 2008;130:2934–2935. [PubMed: 18281995]
25. Marti AA, Puckett CA, Dyer J, Stevens N, Jockusch S, Ju J, Barton JK, Turro NJ. J Am Chem Soc 2007;129:8680. [PubMed: 17592843]
26. Sperschneider J, Datta A. RNA-Publ RNA Soc 2008;14:630–640.
27. Bonnet G, Tyagi S, Libchaber A, Kramer FR. Proc Natl Acad Sci U S A 1999;96:6171–6176. [PubMed: 10339560]
28. Kushon SA, Jordan JP, Seifert JL, Nielsen H, Nielsen PE, Armitage BA. J Am Chem Soc 2001;123:10805–10813. [PubMed: 11686681]
29. Petruska J, Goodman MF. J Biol Chem 1995;270:746–750. [PubMed: 7822305]
30. Du H, Strohsahl CM, Camera J, Miller BL, Krauss TD. J Am Chem Soc 2005;127:7932–7940. [PubMed: 15913384]
31. Jin R, Wu G, Li Z, Mirkin CA, Schatz GC. J Am Chem Soc 2003;125:1643–1654. [PubMed: 12568626]
32. Sauthier ML, Carroll RL, Gorman CB, Franzen S. Langmuir 2002;18:1825–1830.
33. Aboul-ela F, Koh D, Tinoco L Jr, Martin FH. Nucleic Acids Res 1985;13:4811–4824. [PubMed: 4022774]
34. Ikuta S, Takagi K, Wallace BR, Itakura K. Nucleic Acids Res 1987;15:797–811. [PubMed: 3822815]
35. Marky LA, Breslauer KJ. Biopolymers 1987;26:1601–1620. [PubMed: 3663875]
36. (a) Tsourkas A, Behlke MA, Rose SD, Bao G. Nucleic Acids Res 2003;31:1319–1330. [PubMed: 12582252] (b) Ramachandran A, Flinchbaugh J, Ayoubi P, Olah GA, Malayer JR. Biosens Bioelectron 2004;19:727–736. [PubMed: 14709391]
37. Steemers FJ, Ferguson JA, Walt DR. Nature Biotechnol 2000;18:91–94. [PubMed: 10625399]
38. Tsourkas A, Behlke MA, Bao G. Nucleic Acids Res 2002;19:4208–4215. [PubMed: 12364599]
39. Pilcher KE, Fey P, Gaudet P, Kowal AS, Chisholm RL. Nature Protocols 2007;2:1325–1328.

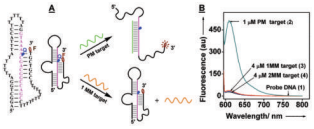

Figure 1.

(A) Mechanism of the SNP sensor. In the presence of a perfectly-matched (PM) target, the folded triple-stem DNA structure is disrupted and fluoresces. In contrast, single-base mismatched (1MM) or two-base mismatched (2MM) targets do not destabilize the discontinuous duplex, and the probe maintains its triple-stem structure with quenched fluorescence. **(B)** Emission spectra of the triple-stem probe (**1**) (0.5 μM) following incubation at room temperature with PM target (**2**), 1MM target (**3**), 2MM target (**4**), or no target. The fluorescence signal was obtained at λ_{ex}= 590 nm and λ_{em}= 610 nm, and all targets were 17 bases in length.

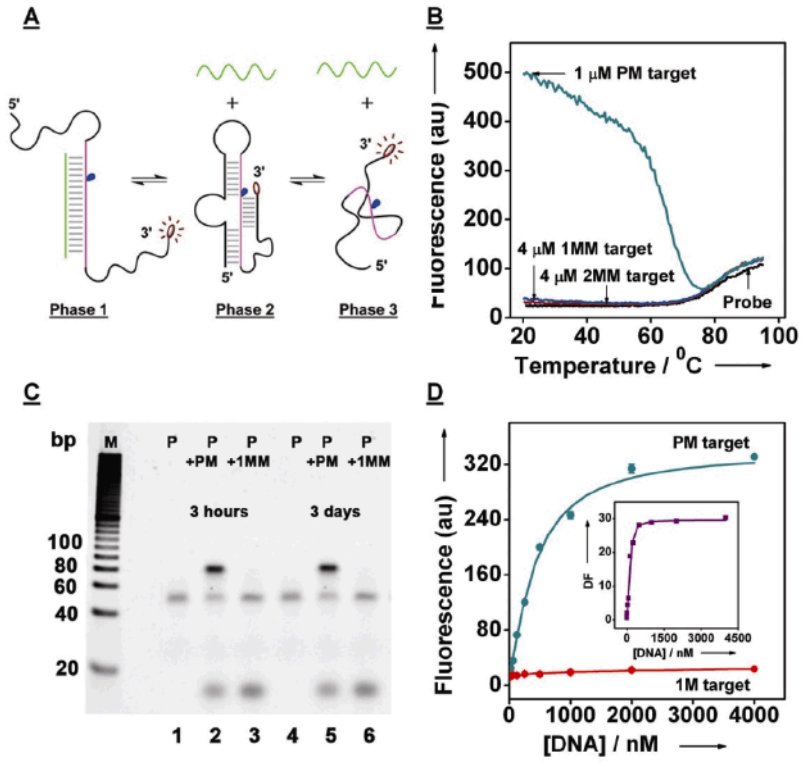

Figure 2.

The triple-stem probe (**1**) displays excellent discrimination against mismatches. **(A)** Proposed phase transitions of the triple-stem probe in the presence of targets at different temperatures. **(B)** The SNP sensor retains its discrimination functionality up to 60 °C. Thermal denaturation curves of the probe only, or hybridized with PM target (**2**), 1MM target (**3**), or 2MM target (**4**). **(C)** Gel image of the triple-stem probe only (lanes 1 and 4), PM target (**2**)-probe samples (lanes 2 and 5) and 1MM target (**3**)-probe samples (lanes 3 and 6). One set of samples was equilibrated for three hours (lanes, 1-3), the other was equilibrated for three days (lanes, 4-6). **(D)** A calibration curve of PM target (**2**) and 1MM target (**3**) for the triple-stem probe. The inset shows the concentration-dependence of discrimination factor of 17-base targets in the presence of 0.5 μM of the probe.

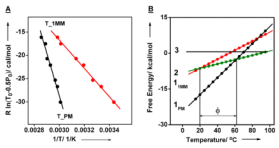

Figure 3.

Determination of thermodynamic parameters. (**A**) The thermodynamic parameters describing the dissociation of probe-target duplexes were determined after measuring the T_m of duplexes that form at variable target concentrations. The determination was performed for triple-stem probe (T) with 17-base PM and 1MM targets. The slope of each fitted line is equal to the negative value of the enthalpy ($-\Delta H_{1\rightarrow 2}^{0}$) and the intercept is equal to the entropy ($\Delta S_{1\rightarrow 2}^{0}$). (**B**) Free energy change for the three phases of a solution of the triple-stem probe in equilibrium with 17-base PM and 1MM targets. The difference (Φ) between the T_m of PM duplexes (1_{PM}) and 1MM duplexes (1_{1MM}) in the triple-stem systems is 43.6 °C.

Table 1

Discrimination factors (DF) of the triple-stem probe (**1**) for single-base mismatched targets differing from the 17-base PM target (**2**) (5'-GCTGGCCGTCGTTTTAC-3') (mismatches marked in red).

DNA Target Sequence (5'---3')	Peak Gain	DF	Mismatched Base-Pair
GCTGGCCGTCGTTTTAC	888.5		
GCTGG**G**CGTCGTTTTAC	113.4	7.8	G-G
GCTGGC**G**GTCGTTTTAC	80.9	10.9	G-G
GCTGGCC**C**TCGTTTTAC	31.3	28.4	C-C
GCTGGCCG**A**CGTTTTAC	159.3	5.6	A-A
GCTGGCCG**C**CGTTTTAC	112.2	7.9	A-C
GCTGGCCG**G**CGTTTTAC	71.6	12.4	A-G
GCTGGCCGT**G**GTTTTAC	61.2	14.5	G-G
GCTGGCCGT**A**GTTTTAC	66.9	13.3	G-A
GCTGGCCGTC**C**TTTTAC	35.0	25.4	C-C
GCTGGCCGTC**A**CTTTAC	55.9	15.8	C-A
GCTGGCCGTCG**C**TTTAC	65.9	13.5	A-C